3-26-2013

Expansion of Breast Cancer Stem Cells with Fibrous Scaffolds

Sheng Feng
University of South Carolina - Columbia, fengs@email.sc.edu

Pang-Kuo Lo
University of South Carolina - Columbia

Shou Liu
University of South Carolina - Columbia, liu282@mailbox.sc.edu

Xinfeng Liu
University of South Carolina - Columbia, xfliu@math.sc.edu

Hexin Chen
University of South Carolina - Columbia, chen53@mailbox.sc.edu

See next page for additional authors

Publication Info
Published in *Integrative Biology*, Volume 5, Issue 5, 2013, pages 768-777.

Integrative Biology

Interdisciplinary approaches for molecular and cellular life sciences

www.rsc.org/ibiology

Volume 5 | Number 5 | May 2013 | Pages 741–836

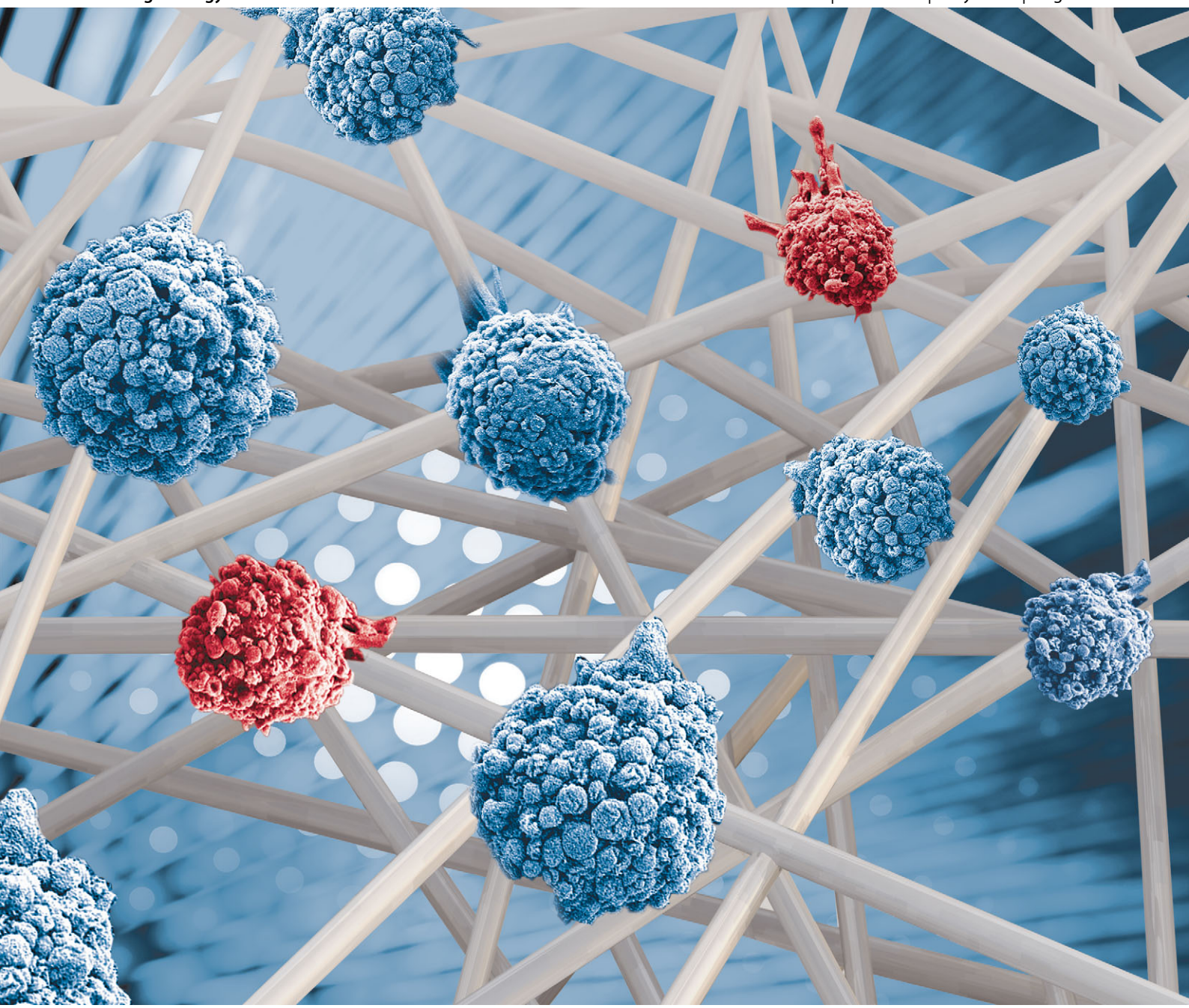

ISSN 1757-9694

RSC Publishing

PAPER

Hexin Chen, Qian Wang *et al.*

Expansion of breast cancer stem cells with fibrous scaffolds

1757-9694(2013)5:5;1-0

Integrative Biology

RSC Publishing

PAPER

View Article Online
View Journal | View Issue

Cite this: *Integr. Biol.*, 2013, **5**, 768

Expansion of breast cancer stem cells with fibrous scaffolds†

Sheng Feng,[a] Xinrui Duan,[a] Pang-Kuo Lo,[b] Shou Liu,[b] Xinfeng Liu,[c] Hexin Chen*[b] and Qian Wang*[a]

Cancer stem cells (CSCs) are hypothesized as tumor-initiating cells within tumors and main contributors of tumor growth, metastasis and recurrence. Mammary cancer cells, MCF-7 cells, were cultured on 3D polycaprolactone (PCL) fibrous scaffolds, showing an increased proportion of CSCs. The expression of stem cell markers, including OCT3/4 and SOX2, and breast CSC-specific markers, SOX4 and CD49f, was significantly upregulated, and the mammosphere-forming capability in cells cultured on PCL fibrous scaffolds increased. The fibrous scaffolds also induced the elongation of MCF-7 cells and extended cell proliferation. The increase of CSC properties after being cultured on fibrous scaffolds was further confirmed with two luminal-type mammary cell lines, T47D and SK-BR-3, and a basal-type cell line, MDA-MB-231, by ALDEFLUOR assay and mammosphere formation assay. Moreover, we observed the upregulation of epithelial to mesenchymal transition and increased invasive capability in cells cultured on PCL fibrous scaffolds. These data suggest that the increase of CSC proportion in a 3D culture system may account for the enhanced malignancy. Therefore, our PCL fibrous scaffolds can potentially be used for CSCs enrichment and anti-cancer drug screening.

Received 19th October 2012,
Accepted 28th February 2013

DOI: 10.1039/c3ib20255k

www.rsc.org/ibiology

Insight, innovation, integration

Three dimensional (3D) culture systems have been utilized in studies of cancer metastasis and anti-tumor drug screening. Accumulating evidence indicates that cancer cells in 3D culture displayed higher malignancy and invasive capability compared to their counterparts in two-dimensional culture. In the present paper, we have fabricated a 3D polycaprolactone fibrous scaffold using an electrospinning process to evaluate how CSCs proportion in breast cancer cell lines responds to this 3D culture. Functional assay and gene profiling together indicate that culture on fibrous scaffolds increased CSCs and induced epithelial-mesenchymal-transition. This work provides a better understanding of how a 3D culture condition affects cancer cells behavior as a mixture of CSCs and non-CSCs. Thus, this knowledge potentially enlightens the design of novel biomaterials for the enrichment of CSCs, and eventually for drug screening targeting CSCs.

Introduction

Cells cultured *in vitro* in two dimensional (2D) tissue culture plastics (TCP) lack the structural architecture necessary for proper cell–cell and cell–matrix interactions that exist *in vivo*.[1–3] The complexity of the *in vivo* system, being composed of many uncontrollable factors, such as immune response, endogenous growth factors, hemodynamics and mechanical cues, complicates research on effects of individual factors on cell behaviours. On the other hand, although rodent animal models are relatively reliable systems for human cancer research and have been used for several decades,[4–7] the significant difference in telomerase regulation between humans and rodents makes transgenic and inducible mouse cancer models questionable in terms of replicating the human cancers.[8] Hence, three-dimensional (3D) cell culture models emerged to bridge the gap between *in vivo* human cancer studies and *in vitro* 2D cell culture models, as well as animal models.

The fabrication of 3D scaffolds for the study of tumor cells *in vitro* has adopted techniques from developed fields of tissue engineering.[1,9,10] Among those techniques, the electrospinning process is a simple and rapid method to generate scaffolds with fibres range from micrometer to nanometer in diameter.[11] Although cells in electrospun fibrous scaffolds often adhere

[a] *Department of Chemistry and Biochemistry, University of South Carolina, Columbia, SC 29208, USA. E-mail: wang263@mailbox.sc.edu*
[b] *Department of Biology, University of South Carolina, Columbia, SC 29208, USA. E-mail: chen53@mailbox.sc.edu*
[c] *Department of Mathematics, University of South Carolina, Columbia, SC 29208, USA*

† Electronic supplementary information (ESI) available. See DOI: 10.1039/c3ib20255k

to the surface with minimum penetration, researchers consider these scaffolds as a 3D-like culture system because cells are able to acquire the nutrition and extracellular signal three dimensionally.[12] Among various natural and synthetic polymers available for the electrospinning process, poly(ε-caprolactone) (PCL) has attracted interest from researchers due to its low melting temperature, good blend-compatibility, FDA approval, and low cost.[13] Nano and microscale fibrous scaffolds obtained by electrospinning are ideal for 3D cell culture, because their structures are similar to components in the extracellular matrix, providing essential cues for cellular survival, proliferation, organization, and function.[12]

Tumor cells grown in 3D scaffolds tend to develop the morphologies and phenotypes observed *in vivo*[14–16] and displayed higher invasive capability, and increased drug resistance relative to cells in a 2D culture condition.[17,18] However, the mechanism of those alterations is still unclear. Recent research has revealed that extracellular matrix (ECM) proteins can be either coated in 2D dishes or fabricated into 3D scaffolds for the enhancement and maintenance of the stemness properties of cancer cells.[19,20]

Cancer stem cells (CSCs) are rare subpopulations that have the capability to initiate tumor growth. Recent research has revealed that CSCs are responsible for metastasis,[21] chemo-resistance,[22] and radio-resistance.[23] In the present study, we hypothesized that the electrospun PCL fibrous scaffolds themselves without any protein component can increase CSCs population. Using aldehyde dehydrogenase (ALDH) activity as a CSCs marker[24] and mammosphere formation assay,[25] we found that MCF-7, T47D, SK-BR-3 and MDA-MB-231 cells cultured on electrospun PCL fibrous scaffolds increased the CSCs population. The enhanced invasiveness and upregulation of epithelial-to-mesenchymal transition (EMT) markers indicate that cells were undergoing EMT, which might trigger the transformation of non-stem cancer cells to CSCs.[26]

Results and discussion

Fabrication of the electrospun PCL fibrous scaffolds

PCL fibrous scaffolds were fabricated using a home-made electrospinning apparatus. For electrospun scaffolds to be reproduced, the important parameters of electrospinning were recorded and illustrated (Fig. 1a). With a stationary collector placed at 10 cm underneath the tip, random fibrous scaffolds were obtained, and no preferred fibre orientation was observed under scanning electron microscope (SEM) (Fig. 1b). The average fibre diameter calculated by Image J software was 1.63 ± 0.36 μm and the diameter distribution of this PCL scaffold ranged from 0.76 to 2.35 μm (Fig. 1c).

Although in diseases or during the movement, the ECM will be reorganized in aligned orientation, the major component of ECM, collagen fibres, usually randomly surrounded the breast epithelial cells,[27] which is similar to the organization of the electrospun PCL random fibrous scaffolds. Our lab found that luminal-type cell line MCF-7 maintained cell–cell contact and random orientation on aligned fibrous scaffolds, indicating less impacts of the aligned fibre on the cells.[28] The aligned fibre orientation will introduce the mechanical stretch on the cells, which might complicate the interpretation of results. Therefore, in this study we use random orientation fibrous scaffolds for cell culture.

Cellular morphology and growth on electrospun PCL 3D scaffolds

MCF-7 cells successfully propagated on PCL fibrous scaffolds. Fluorescence microscopy revealed different morphologies between MCF-7 cells cultured on electrospun PCL fibrous scaffolds and TCP (Fig. 2). Cells on TCP exhibited trigonal or polygonal morphologies, whereas cells on PCL fibrous scaffolds showed round shuttle-like shape. We also observed similar results in T47D, SK-BR-3, and MDA-MB-231 cells (Fig. S1, ESI†). Relative to cells on TCP with a spreading-out morphology, cells on PCL fibrous scaffolds displayed a smaller F-actin staining area and round-like shape. This might be because fibres surrounding cells limited cells spreading and cells increased in thickness (Fig. S2, ESI†).

We utilized CellTiter-Blue assay to measure cell growth on PCL scaffolds. On day 7, MCF-7 cells on TCP and fibrous scaffolds proliferated to 15.00 ± 0.48-fold and 13.87 ± 0.56-fold relative to day 1, respectively. There was no statistically significant difference in the proliferation rate between cells on TCP and PCL fibrous scaffolds during the first 7 days. However, on day 9, cells cultured on TCP reached a plateau, whereas cells

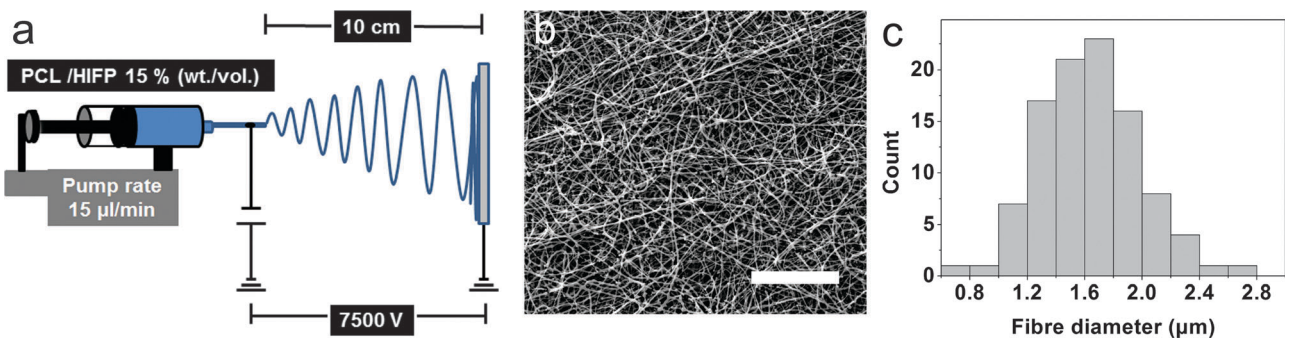

Fig. 1 PCL fibrous scaffolds were fabricated by the electrospinning process. (a) The schematic illustration of electrospinning setup. (b) The SEM image of the electrospun PCL fibrous scaffold. Scale bar indicates 100 μm. (c) The distribution of the fiber diameter on PCL fibrous scaffolds fabricated in the described setting.

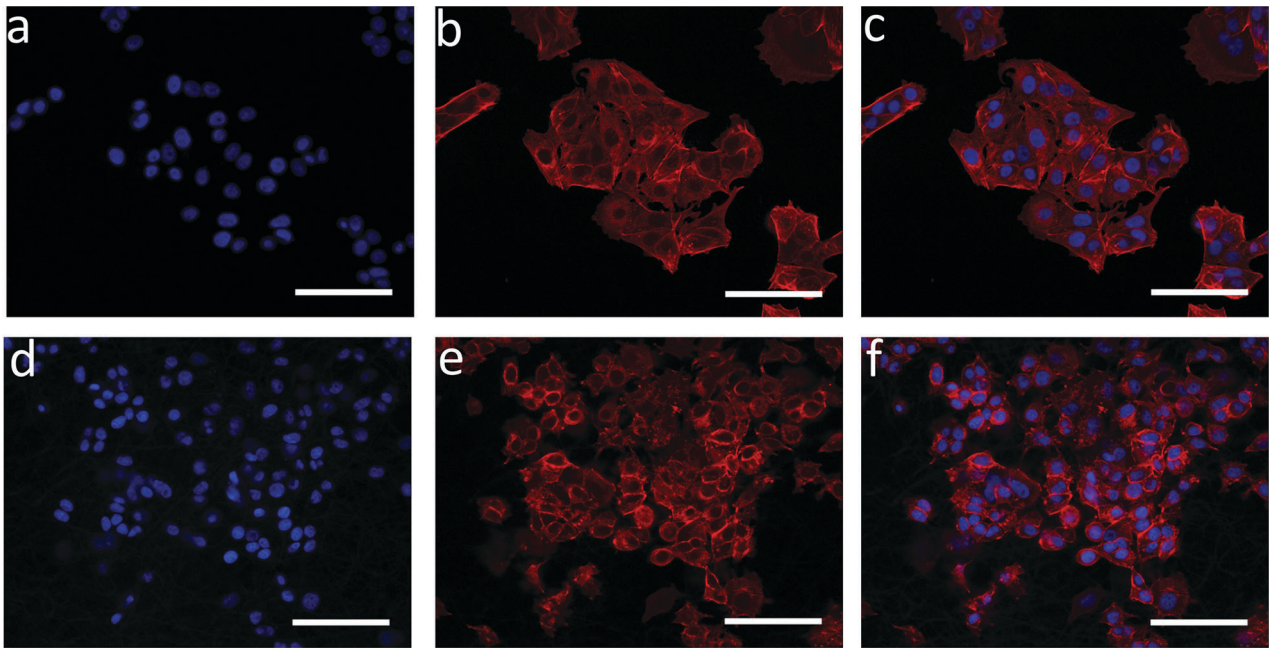

Fig. 2 Fluorescence microscopy images of MCF-7 cells cultured in 2D tissue culture plastics (a–c) and 3D PCL fibrous scaffolds (d–f). Blue indicates nuclei (DAPI); red indicates F-actin (rhodamine-phalloidin). All scale bars indicate 100 μm.

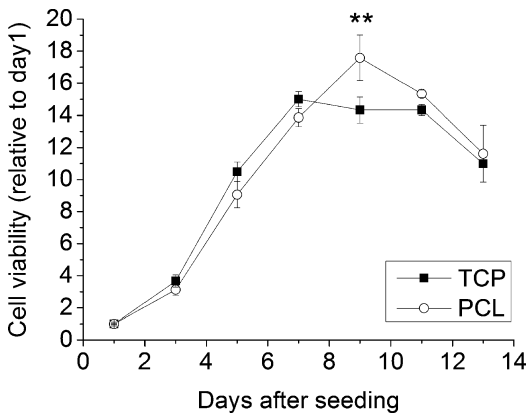

Fig. 3 The proliferations of MCF-7 in 2D tissue culture plastics (TCP) and 3D PCL fibrous scaffolds (PCL) were measured at indicated time points by CellTiter-Blue assay. Results were shown as mean ± standard deviation. Statistical significance of the differences between cells on TCP and PCL is indicated by two asterisks ($P < 0.005$, $n = 3$).

on PCL fibrous scaffolds continued propagating to 17.58 ± 1.43-fold relative to day 1 (Fig. 3). Considering the seeding cell densities were the same in these two culture systems, the discrepancy might come from the expanding space for cell growth in 3D PCL fibrous scaffolds, because some of the cells migrated through the pores and grew under layers of the fibres (Movie S1, ESI†). We also observed a similar trend in MDA-MB-231 cells (Fig. S3, ESI†).

Culturing breast cancer cell lines on PCL fibrous scaffolds induces the expansion of the CSC subpopulation

The CSC theory postulates that a small group of cells, which is selected by specific combination of markers, are responsible for the initiation and maintenance of tumors. Chen and his colleagues found that MCF-7 cells in 3D collagen scaffolds displayed enhanced stemness relative to their counterparts in 2D culture.[20] The collagen scaffolds provide not only a 3D culture scaffold, but also a microenvironment with protein–protein interactions between membrane proteins of MCF-7 cells and collagen. In this study, the unmodified electrospun PCL scaffolds exclude the protein–protein interaction between cells and scaffolds. We cultured MCF-7 cells on PCL fibrous scaffolds to test how this fibrous scaffold culture condition affects the size of CSCs population.

Aldehyde dehydrogenase, which is a detoxifying enzyme responsible for the oxidation of intracellular aldehyde, may play a role in early differentiation of stem cells through its role in oxidizing retinol to retinoic acid.[29] Accumulating data indicates that ALDH expression is related to cells with enhanced tumorigenic and metastatic potential.[30–32] In addition, based on ALDH activity, Ginestier and colleagues successfully isolated CSCs from human breast tumors, and the expression of ALDH1 was considered as a predictor of clinical outcomes in breast cancer patients.[24] We utilized the ALDEFLUOR assay to assess the proportion of CSCs in breast cancer cells from PCL fibrous scaffolds and TCP respectively.[33] The ratio of ALDH-positive population of MCF-7 cells increased to 6.33 ± 0.55% in 3D PCL scaffolds relative to 2.00 ± 0.04% in 2D TCP after 6 days culture without passage (Fig. 4a and d). We also assessed CSCs in two other luminal-type cell lines, T47D and SK-BR-3, from PCL fibrous scaffolds and TCP. The proportion of ALDH-positive cells in T47D and SK-BR-3 increased to 6.80 ± 0.58% and 18.27 ± 1.73% on PCL fibrous scaffolds from 1.82 ± 0.74% and 7.22 ± 0.19% on TCP, respectively (Fig. 4).

Previous research reported that mammary epithelial stem and progenitor cells can survive and propagate in an

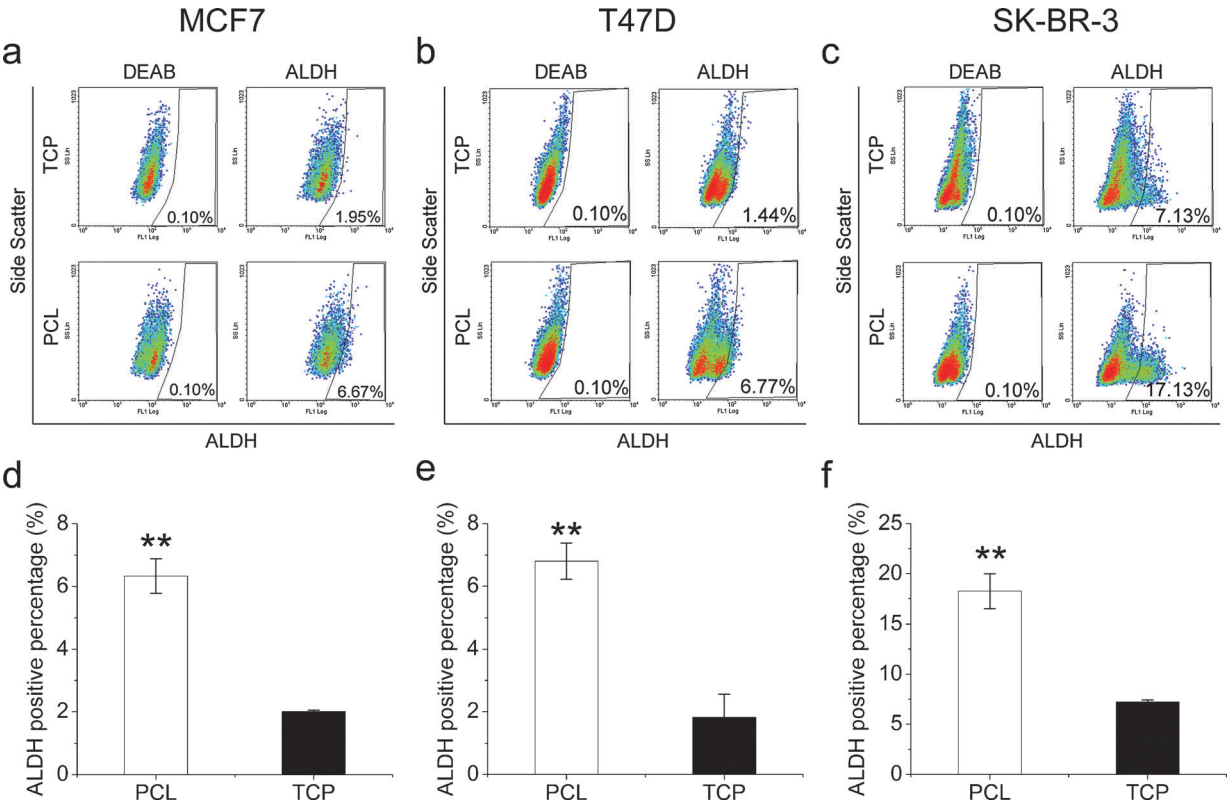

Fig. 4 Epithelial breast cancer cell lines, MCF-7, T47D, and SK-BR-3 cultured on PCL fibrous scaffolds (PCL) increased ALDH-positive population compared with counterparts cultured on TCP. (a–c) After being cultured for 6 days on PCL and TCP without passage, cells were harvested and analyzed by ALDEFLUOR assay. The ALDH inhibitor, diethylaminobenzaldehyde (DEAB) (15 μM), was added to the cell suspension in the ALDEFLUOR assay buffer with the substrate as a negative control. Numbers indicate the percentages of cells in the gated area. (d–f) The percentage of ALDH-positive cells in MCF-7, T47D, and SK-BR-3 cells cultured on PCL and TCP. Results were shown as mean ± standard deviation. Statistical significance is indicated by double asterisks ($P < 0.001$, $n = 3$).

attachment-independent manner and form floating spherical colonies, which are termed mammospheres.[25] Therefore the mammosphere formation assay is often used to identify and enrich CSCs. To further confirm whether the PCL fibrous scaffolds culture system increases the size of CSCs population, we measured the mammosphere formation ability of MCF-7 cells from TCP and PCL fibrous scaffolds. We found that the MCF-7 cells from PCL fibrous scaffolds formed approximately 2.0-fold more mammospheres than control cells from TCP (Fig. 5a). The sphere formation efficiency of T47D and SK-BR-3 from PCL fibrous scaffolds increased to 1.81 ± 1.07% and 3.44 ± 0.42%, relative to 1.07 ± 0.50% and 2.51 ± 0.16% for cells on TCP, respectively (Fig. 5b and c). Some of those spheres have a large size of around 100 μm. These spheres probably came from multiple cells fusion.[34,35] Those data suggests that CSCs expanded in those mammary cancer cell lines when cultured in electrospun PCL fibrous scaffolds.

OCT3/4 and SOX2 function cooperatively to regulate their own transcription and the transcription of a large set of other genes, which control the self-renewal and pluripotency of stem cells.[36] SOX4 functions in the progression of breast cancer by orchestrating EMT.[37] CD49f has been used for enrichment of normal cells and CSCs,[38,39] which maintains the pluripotency and stemness through the direct regulation of OCT4 and SOX2.[40] In our study, transcriptional factors related to stem cells, including SOX2 and OCT3/4, and breast CSC signatures, including SOX4 and CD49f, were enhanced in MCF-7 cultured on fibrous scaffolds by 1.77 ± 0.25-fold, 2.22 ± 0.23-fold, 1.56 ± 0.25-fold, and 2.92 ± 0.33-fold, respectively, relative to cells on TCP (Fig. 5a). In addition, among stemness related genes, only SOX2 were upregulated in T47D from PCL fibrous scaffolds, while OCT3/4, SOX2, and CD49f were upregulated in SK-BR-3 cells from PCL fibrous scaffolds, relative to cells from TCP (Fig. 5b).

To investigate whether the effect of 3D PCL fibrous scaffolds culture on CSCs expansion is cell-phenotype specific, we examined how CSCs respond to the fibrous scaffold culture in a highly malignant basal-type cell line, MDA-MB-231 cells. ALDEFLUOR assay, mammosphere formation assay, and gene expression patterns all show that MDA-MB-231 cells on PCL fibrous scaffolds increased CSCs population relative to cells on TCP (Fig. S9, ESI†). Although the proportion of CSCs in MDA-MB-231 cells cultured on PCL fibrous scaffolds increases not as dramatically as in epithelial cell lines, the same trend of changes in the CSC population in several breast cancer cell lines cultured indicates that this phenomenon is not cell-phenotype specific.

Studies have demonstrated that tumor cells cultured in 3D systems displayed properties of increased malignancy and drug

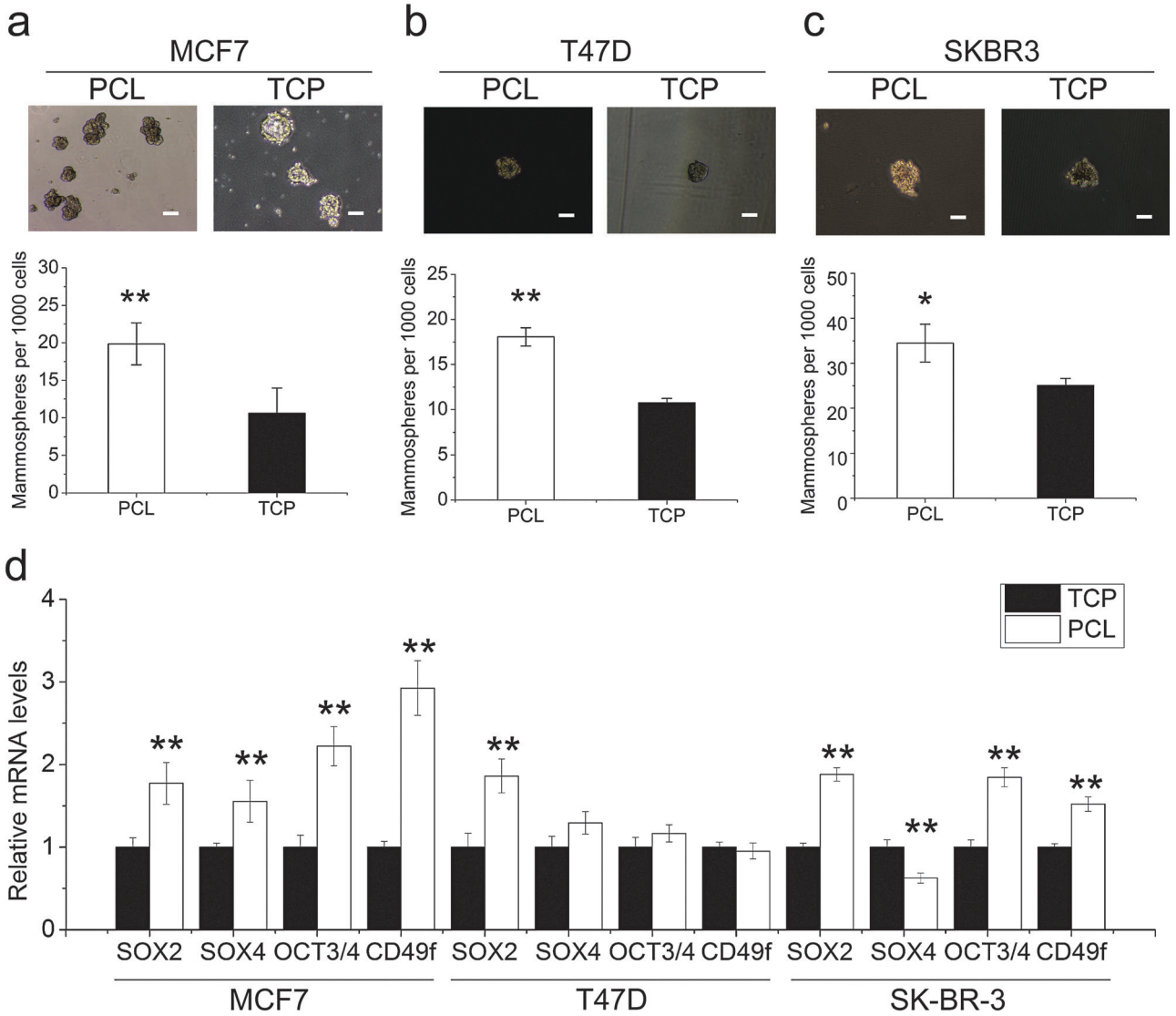

Fig. 5 Epithelial breast cancer cell lines, MCF7, T47D, and SK-BR-3 on PCL fibrous scaffolds (PCL) increased the property of stemness. (a–c) Cells cultured on PCL and TCP for 6 days without passage were harvested for mammoshpere formation assay. Mammospheres were observed under microscopy and enumerated. Results are shown as mean ± standard deviation. Statistical significance is indicated by single asterisk ($P < 0.05$, $n = 6$) or double asterisks ($P < 0.005$, $n = 6$). Scale bars indicate 100 μm. (d) SOX2, SOX4, OCT3/4, and CD49f expression in MCF-7, T47D, and SK-BR-3 cultured on PCL and TCP. Results are shown as mean ± standard deviation. Statistical significance is indicated by a single asterisk ($P < 0.05$, $n = 3$) or double asterisks ($P < 0.005$, $n = 3$).

resistance compared to standard 2D cultured tumor cells.[16,18,41,42] Given the fact that CSCs are responsible for metastasis and drug resistance, the expansion of CSCs in tumor cells cultured in 3D may account for this change.

The enhancement of EMT-associated properties in cells from PCL fibrous scaffolds

The EMT is a developmental process, in which epithelial cells with tight cell junctions and relatively low migratory ability convert to mesenchymal cells with migratory and invasive phenotype. Recent studies demonstrate that during the carcinoma progression, some tumor cells are undergoing the EMT.[43] The inducing factors of EMT include growth factors, cell–matrix interaction, and hypoxia. In addition, EMT may also trigger the transformation of non-stem cancer cells to CSCs, in which tumor cells are acquiring properties of invasion, drug-resistance, chemo-resistance, and radio-resistance.[26]

We previously reported that culture on PCL fibrous scaffolds with either aligned fibres or random fibres can stimulate mouse mammary cell line H605 to undergo EMT.[28] Here, we investigated whether human epithelial-type breast cancer cell lines MCF-7, T47D, and SK-BR-3 cultured on PCL fibrous scaffolds were undergoing EMT.

A classical definition of EMT is a multiple step process, in which cells acquire a mesenchymal morphology and then demonstrate increased migration and invasion.[44] MCF-7 cells from PCL fibrous scaffolds were reseeded to TCP, of which about 10% demonstrated elongated spindle-like morphology (Fig. S5, ESI†). There was no morphological change for reseeded T47D and SK-BR-3 cells from fibrous scaffolds. Using Transwell assay,

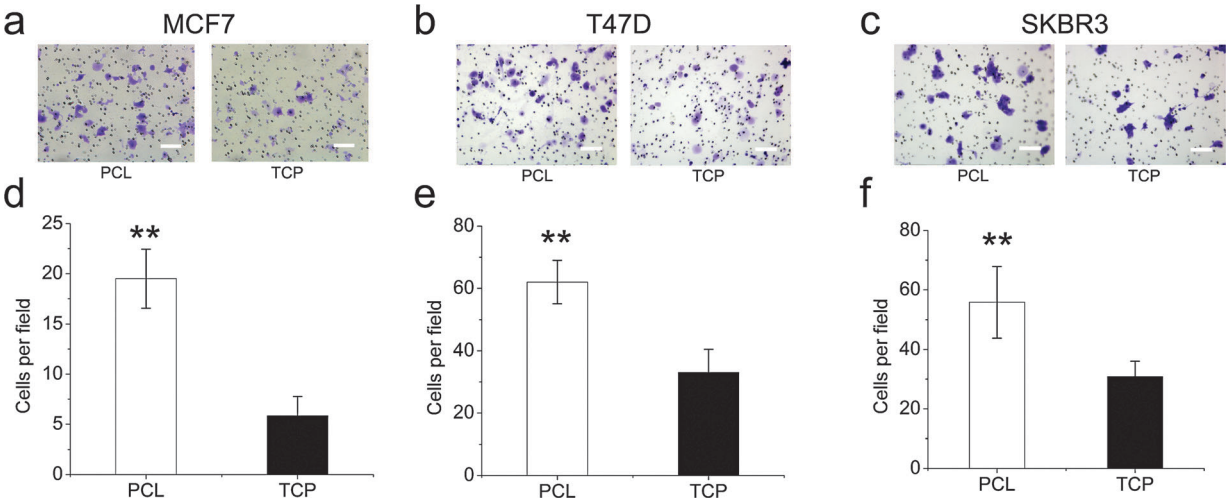

Fig. 6 Culture on PCL fibrous scaffolds (PCL) increases the invasion of MCF-7, T47D, and SK-BR-3 cells. (a–c) MCF-7, T47D, SK-BR-3 cells from PCL displayed higher invasive capability in the Transwell invasion assay compared to counterparts from TCP. Cells that successfully migrated through the filter pores were fixed with 3.7% paraformaldehyde and stained with 0.5% crystal violet in 2% ethanol. Scale bars indicate 100 μm. (d–f) The average number of migrated cells per field was assessed by counting six random fields. Statistical significance is indicated by double asterisks ($P < 0.001$, $n = 3$).

we measured the invasive property of MCF-7, T47D, and SK-BR-3 cells, a characteristic associated with EMT. Cells from PCL fibrous scaffolds showed significant increases in the number of cells passing through the membrane (Fig. 6).

To further confirm that cells on PCL fibrous scaffolds were undergoing EMT, we measured the transcriptions of EMT related genes in cells from two different culture conditions. The expression of EMT related transcriptional factors, including SLUG, SNAIL, TWIST1, TWIST2, ZEB1, ZEB2, and FOXC2, and other EMT markers, including VIM and ITGA5, were significantly upregulated in MCF-7 cells on PCL fibrous scaffolds in comparison with cells cultured on TCP (Fig. 6b). In T47D cells on PCL fibrous scaffolds, EMT related transcriptional factors, SNAIL, TWIST1, TWIST2, and ZEB2 were upregulated, compared to cells on TCP. In SK-BR-3 cells, only ZEB2, VIM, and ITGA5 were upregulated. Meanwhile, the expression of the epithelial marker, CDH-1 (E-cadherin), decreased in cells from PCL fibrous scaffolds relative to cells from TCP. Indirect immunofluorescence staining of cells with E-cadherin antibody revealed that most of the cells, if not all, on fibrous scaffolds still expressed E-cadherin protein (Fig. S6, ESI†). Western blot analysis indicates that there is no significant change in protein level for E-cadherin and vimentin in cells from fibrous scaffolds relative to cells from TCP (Fig. S8, ESI†). It is probably because the cells are still undergoing the early transition of EMT, which is a relatively slow process. For example, TGF-β normally induces EMT within about two weeks.[45] The improvement of invasion and enhancement of expression of EMT markers suggests cells on PCL fibrous scaffolds were undergoing EMT (Fig. 7).

It was reported that immortalized human mammary epithelial cells undergoing EMT displayed a shift in CD44 expression from variant isoforms (CD44v) to the standard form (CD44s).[46] In the present study, we observed that CD44v, CD44s and CD44t were all upregulated in cells cultured on PCL fibrous scaffolds (Fig. S4, ESI†). CD24 regulates TGF-β3 and E-cadherin in oral epithelial cells during EMT.[47] The downregulation of CD24 and the upregulation of TGF-β3 in cells cultured on fibrous scaffolds suggest that cells were undergoing EMT (Fig. S4, ESI†).

MDA-MB-231 cells have basal-like properties and possess mesenchymal phenotype due to high expression of vimentin.[48,49] Indeed, the basal level of the EMT related gene in MDA-MB-231 cells is higher than in epithelial-like cells, MCF7, T47D, and SK-BR-3. Culture on fibrous scaffolds further enhances the expression of EMT related genes in MDA-MB-231 cells (Fig. S9, ESI†). It is acknowledged that the EMT process is related to stemness.[26] If the increased CSCs came from the transformation of non-stem cancer cells induced by EMT, CSCs proportion in the mesenchymal-type cell line, MDA-MB-231, would not change as dramatically as the epithelial-type cell lines, because the mesenchymal cell line cannot undergo the EMT process.

A previous study suggested that MCF-7 cells on 3D collagen scaffolds were induced to undergo EMT may be due to the adaption to the hypoxia condition.[50] In our study most of the cells localized on the surface of scaffolds, and a few cells infiltrated into the lower layers, which is not sufficient to induce the hypoxia condition. Therefore it might be other factors rather than hypoxia that induced cells to undergo EMT in this case. It is acknowledged that compressive forces generated by the interaction between cells and their surrounding environment can cause, either directly or indirectly, alterations of cell in the structure and function of ECM receptors to actively influence the signaling pathway. EMT in the tumor environment is a force-dependent phenomenon.[51] TGF-β studies revealed that dynamic compression and contraction of cell–matrix interaction activates latent ECM bound TGF-β, thereby stimulating a feedback loop to induce EMT in the cell itself.[52,53] Further research will be required to elucidate

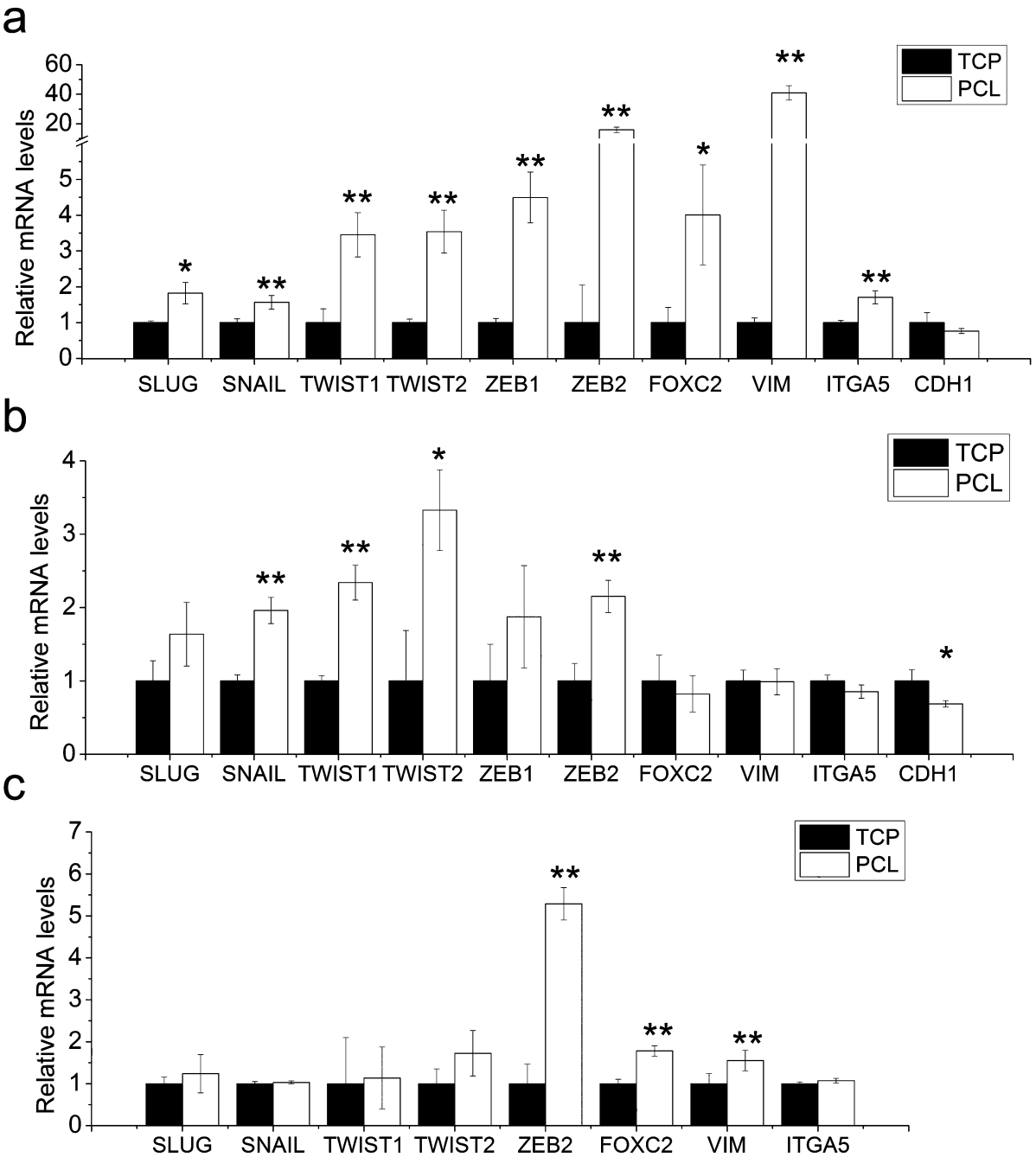

Fig. 7 PCL fibrous scaffolds culture enhanced the expression of EMT related markers. Differential expressions of EMT markers were measured by qRT-PCR in MCF-7 (a), T47D (b), and SK-BR-3 (c) from PCL and TCP. Results were shown as mean ± standard deviation. Statistical significance is indicated by single asterisk ($P < 0.05$, $n = 3$) or double asterisks ($P < 0.005$, $n = 3$).

the detailed mechanism of how the 3D PCL fibrous scaffolds induce cells to undergo EMT.

Although EMT can induce the conversion of non-stem cancer cells to CSCs, a recent study suggests EMT and stemness are not necessarily linked.[54] In the present study, we found that PCL fibrous scaffolds culture conditions increased CSCs properties and induced EMT. However, it is still unclear whether that EMT and the increase of CSCs are two independent events or two events with causal relationship. Further work needs to be done to understand the relationship between EMT and the increase of CSCs in electrospun PCL fibrous scaffolds.

Experimental

Preparation of electrospun PCL fibrous scaffolds

A 15% w/w solution of poly(ε-caprolactone) (PCL) (Average M_n *ca.* 60 kDa, Sigma), in 1,1,1,3,3,3-hexafluro-2-propanol (HFIP) (Sigma Aldrich) was made. The electrospinning system is placed

in a humidity-controlled chamber and schematically depicted in Fig. 1a. The electrospinning process was conducted as follows: the polymer solution was transferred to a 1.0 mL plastic syringe (BD) with a 21 G blunt needle (BD precision glide). A syringe driver was used to control the solution flow rate at 15 μL min^{-1}. A high voltage supply (HVR Orlando, FL) was used to build up a voltage of 6–7 kV electro filed between the needle and the grounded collector. The distance between the collector and needle was fixed at 10 cm. The PCL fibrous scaffold was fertilized by immersing into 75% ethanol for 20 min, dried overnight and then irradiated under ultraviolet light for 20 min in a laminar flow hood.

Cell culture

Human breast cancer cell lines MCF-7, T47D, SK-BR-3, and MB-MDA-231 were purchased from the American Type Culture Collection. MCF-7 and MDA-MB-231 cells were cultured in Dulbecco's modified Eagle's medium (DMEM, #D6046, Sigma-Aldrich) supplemented with 10% heat inactivated fetal bovine serum (Hyclone, Thermo Scientific), 100 U mL^{-1} penicillin and 100 μg mL^{-1} streptomycin (Gibco BRL, Invitrogen Corp., Carlsbad, CA, USA). T47D was maintained in RPMI-1604 media (Sigma-Aldrich) containing 10% FBS, 100 U mL^{-1} penicillin and 100 μg mL^{-1} streptomycin. SK-BR-3 was maintained in KBR3 cells grown in McCoy's 5A (Sigma-Aldrich) supplemented with 10% FBS, 10% FBS and 100 U mL^{-1} penicillin and 100 μg mL^{-1} streptomycin. Cells were cultured in a 5% CO_2 humidified incubator at 37 °C. Sterilized PCL fibre scaffolds were soaked in media 30 min prior to cell seeding. Cells in the exponential growth phase were trypsinized using 0.25% trypsin and seeded on a PCL fibrous scaffold at a density of 5.2×10^3 cells per cm^2. The cells used in experiments were cultured on PCL and TCP for 6 days without passage, unless otherwise specified.

Confocal and scanning electron microscopy studies

Cells on PCL fibre scaffolds were rinsed with phosphate buffered saline (PBS) twice and fixed with 4% paraformaldehyde for 20 min at room temperature. Then scaffolds were rinsed with PBS. Cells were permeabilized with 0.2% Triton X-100 for 10 min. To prevent non-specific labeling, 3% bovine serum albumin (BSA) in PBS was applied as a blocking buffer for 20 min. Actin cytoskeleton was stained with rhodamine phalloidin (Cytoskeleton Inc.) (1 : 200) in a blocking buffer for 20 min, and nuclei were stained with 4′,6-diamidino-2-phenylindole (DAPI) (Invitrogen) in a blocking buffer for 10 min. The fluorescence was visualized and captured under confocal microscope (Olympus IX81) with DAPI filter and Cy3 filter set. The morphologies of PCL fibre scaffolds were examined using a field emission scanning electron microscope (FEI Quanta 200 ESEM). PCL scaffold samples were dried with nitrogen, and coated with gold for 30 seconds with sputter coater. To examine the uniformity of the fibre diameters several areas were imaged. Fibre diameters were measured using image J (National Institutes of Health).

ALDEFLUOR assay

The ALDEFLUOR kit (Stem Cell Technologies, Durham, NC, USA) was used to identify the cancer stem cell population with high ALDH enzyme activity. Briefly, the cells were suspended in ALDEFLUOR assay buffer containing ALDH substrate BAAA (1 μM) at a concentration of 1×10^6 cells per mL^{-1} and incubated for 45 min at 37 °C. As a negative control, the ALDH inhibitor, diethylaminobenzaldehyde (DEAB) (15 μM), was added to the cell suspension in ALDEFLUOR assay buffer with BAAA. A Cytomics FC500 flow cytometry system (Beckman Coulter Inc., Miami, FL, USA) was used to detect the ALDH-positive cell population.

Cell proliferation assay

The effect of PCL fibre scaffolds on cell growth was assessed by CellTiter-Blue™ Cell Viability Assay (Promega, Madison, WI). The cell titer blue reagent was added to the medium directly (100 μL per 1 mL medium) and incubated for four hours at 37 °C. Fluorescence at $560_{ex}/590_{em}$ nm filter setting was measured using a Tecan infinite M200 plate reader (Tecan, Salzburg, Austria). After correction of background fluorescence, the intensity of fluorescence for each sample was normalized by the first day intensity of fluorescence. The cell viabilities at days 1, 3, 5, 7, 9, 11, and 13 were determined. Three independent experiments were determined for each case.

Mammosphere formation assay

Cells from 2D culture or 3D PCL fibrous scaffolds were plated in ultralow attachment six-well plates (Corning, Acton, MA, USA) at a density of 10 000 cells per mL^{-1} for MCF-7 and 1000 cells per mL^{-1} for MDA-MB-231 in serum-free DMEM/F12 medium (Invitrogen, Carlsbad, CA, USA) supplemented with 20 ng mL^{-1} epidermal growth factor (Sigma, St Louis, MO, USA), 10 ng mL^{-1} basic fibroblast growth factor (Sigma), 5 μg mL^{-1} insulin (Sigma), 1 × B27 supplement (Invitrogen) and 0.4% bovine serum albumin (Sigma). Cells were cultured in a 5% CO_2 humidified incubator at 37 °C for a week. The number of mammospheres was counted under microscopy. Three independent experiments were performed for each group.

RNA extraction and quantitative reverse-transcription PCR

Total RNA was isolated using an RNeasy mini purification kit (Qiagen). Quantitative reverse-transcription PCR (qRT-PCR) was performed in two steps. Isolated RNA was reverse-transcribed using a qScript™ cDNA synthesis kit (Quanta Biosciences Inc.) and then Quantitative (real-time) PCR was performed using a Bio-Rad iCycler with a My iQ™ camera detection system and the method used was 40 cycles of PCR (95 °C for 30 s, 60 °C for 15 s, 72 °C for 30 s), after an initial denaturation step of 5 min at 95 °C. In a 25 μL total volume of the reaction mixture, 12.5 μL iQ SYBR-Green™ SuperMix (Bio-Rad), 400 nM of both forward and reverse primers (Table S1, ESI†) and the cDNA template at a final concentration of 25 ng μL^{-1} were employed. Data analysis was performed using the $2^{-\Delta\Delta C}T$ method for relative quantification,[55] and all samples were normalized to GAPDH expression as the internal control.

Transwell invasion assay

The invasion chamber consisted of a cell culture insert with a membrane pore size of 8 μm in a 24-well plate (BD Biocoat™

Matrigel™ Invasion Chamber, BD Biosciences, Franklin Lakes, NJ). Cells cultured in 2D and 3D were trypsinized and washed by PBS. Then cells were plated in the top chamber with Matrigel-coated membrane at a density of 2.5×10^5 cells per well for MCF-7 and 1×10^6 cells per well for SK-BR-3 and T47D. Cells were plated in the serum free medium and medium with 10% FBS was used as a chemoattractant in the lower chamber. The cells were incubated in a 5% CO_2 humidified incubator at 37 °C for 72 h. Cells that fail to invade through pores were removed using a cotton swab. Cells on the lower surface of the membrane were fixed with 3.7% paraformaldehyde and stained with 0.5% crystal violet in 2% ethanol and counted under a microscope.

Statistical analysis

All assays were performed in triplicate unless otherwise stated. Data are indicated as mean ± standard deviation. Comparisons between two groups were done using unpaired Student's *t*-test.

Conclusions

Cancer stem cells, which are responsible for the tumorigenesis, chemo-resistance, radio-resistance, and metastases, play a vital role in the tumor initiation and regression. Previous studies suggested that cells in traditional 2D culture fail to represent *in vivo* tumor cells, due to the loss of the malignancy. In the present study, using the electrospinning process, we generated PCL fibrous scaffolds for 3D cell culture. Three epithelial-type breast cancer cell lines, including MCF-7, T47D, SK-BR-3, cultured on PCL fibrous scaffolds showed increased CSCs population relative to cells cultured on TCP, which may likely attribute to the EMT process.

Recently we have developed a set of mathematical models with two negative feedbacks to explore essential biological factors that control the CSC population during tumor growth, in which an excellent agreement with experimental data has been achieved. To characterize the underlying features of CSCs induced by 3D PCL fibrous scaffolds, we plan next to extend mathematical models as proposed by including the transformation from non-stem cells to CSCs to further investigate whether the enrichment of CSCs by 3D PCL fibre scaffolds is primarily due to transformation of non-stem cells to CSCs, or increasing symmetric division or differentiation rates of CSCs, or the combination of these different factors. With this data, we anticipated that PCL fibrous scaffolds culture system, in which cells demonstrate higher malignancy and the expansion of CSCs, could be used as a useful scaffold for the evaluation of novel anti-cancer drugs and the enrichment of cancer stem cells *in vitro*.

Acknowledgements

We gratefully acknowledge the financial support of this work by NIH grant (3P20RR017698-08) to HC and QW, the American Cancer Society Research Award (RSG-10-067-01-TBE) to HC, and the support to QW from the US NSF CHE-0748690 and the Camille Dreyfus Teacher Scholar Award.

References

1 J. B. Kim, *Semin. Cancer Biol.*, 2005, **15**, 365–377.
2 L. G. Griffith and M. A. Swartz, *Nat. Rev. Mol. Cell Biol.*, 2006, **7**, 211–224.
3 C. S. Szot, C. F. Buchanan, J. W. Freeman and M. N. Rylander, *Biomaterials*, 2011, **32**, 7905–7912.
4 V. N. Anisimov, S. V. Ukraintseva and A. I. Yashin, *Nat. Rev. Cancer*, 2005, **5**, 807–819.
5 A. Rangarajan and R. A. Weinberg, *Nat. Rev. Cancer*, 2003, **3**, 952–959.
6 A. F. Frijhoff, C. J. Conti and A. M. Senderowicz, *Mol. Carcinog.*, 2004, **39**, 183–194.
7 G. M. de Jong, F. Aarts, T. Hendriks, O. C. Boerman and R. P. Bleichrodt, *J. Surg. Res.*, 2009, **154**, 167–176.
8 A. Rangarajan, S. J. Hong, A. Gifford and R. A. Weinberg, *Cancer Cell*, 2004, **6**, 171–183.
9 O. Hartman, C. Zhang, E. L. Adams, M. C. Farach-Carson, N. J. Petrelli, B. D. Chase and J. F. Rabolt, *Biomaterials*, 2010, **31**, 5700–5718.
10 C. S. Szot, C. F. Buchanan, P. Gatenholm, M. N. Rylander and J. W. Freeman, *Mater. Sci. Eng., C*, 2011, **31**, 37–42.
11 D. Han and P. I. Gouma, *Nanomedicine*, 2006, **2**, 37–41.
12 D. R. Nisbet, J. S. Forsythe, W. Shen, D. I. Finkelstein and M. K. Horne, *J. Biomater. Appl.*, 2009, **24**, 7–29.
13 A. Cipitria, A. Skelton, T. R. Dargaville, P. D. Dalton and D. W. Hutmacher, *J. Mater. Chem.*, 2011, **21**, 9419.
14 K. M. Yamada and E. Cukierman, *Cell*, 2007, **130**, 601–610.
15 X. Wang, L. Sun, M. V. Maffini, A. Soto, C. Sonnenschein and D. L. Kaplan, *Biomaterials*, 2010, **31**, 3920–3929.
16 C. Fischbach, R. Chen, T. Matsumoto, T. Schmelzle, J. S. Brugge, P. J. Polverini and D. J. Mooney, *Nat. Methods*, 2007, **4**, 855–860.
17 M. A. D. Faute, L. Laurent, D. Ploton, M. F. Poupon, J. C. Jardillier and H. Bobichon, *Clin. Exp. Metastasis*, 2002, **19**, 161–168.
18 M. Leung, F. M. Kievit, S. J. Florczyk, O. Veiseh, J. Wu, J. O. Park and M. Zhang, *Pharm. Res.*, 2010, **27**, 1939–1948.
19 S. M. Pollard, K. Yoshikawa, I. D. Clarke, D. Danovi, S. Stricker, R. Russell, J. Bayani, R. Head, M. Lee, M. Bernstein, J. A. Squire, A. Smith and P. Dirks, *Cell Stem Cell*, 2009, **4**, 568–580.
20 S. Saha, P.-K. Lo, X. Duan, H. Chen and Q. Wang, *Integr. Biol.*, 2012, **4**, 897–904.
21 B. K. Abraham, P. Fritz, M. McClellan, P. Hauptvogel, M. Athelogou and H. Brauch, *Clin. Cancer Res.*, 2005, **11**, 1154–1159.
22 X. X. Li, M. T. Lewis, J. Huang, C. Gutierrez, C. K. Osborne, M. F. Wu, S. G. Hilsenbeck, A. Pavlick, X. M. Zhang, G. C. Chamness, H. Wong, J. Rosen and J. C. Chang, *J. Natl. Cancer Inst.*, 2008, **100**, 672–679.
23 M. Diehn, R. W. Cho, N. A. Lobo, T. Kalisky, M. J. Dorie, A. N. Kulp, D. L. Qian, J. S. Lam, L. E. Ailles, M. Z. Wong,

B. Joshua, M. J. Kaplan, I. Wapnir, F. M. Dirbas, G. Somlo, C. Garberoglio, B. Paz, J. Shen, S. K. Lau, S. R. Quake, J. M. Brown, I. L. Weissman and M. F. Clarke, *Nature*, 2009, **458**, 780–783.

24 C. Ginestier, M. H. Hur, E. Charafe-Jauffret, F. Monville, J. Dutcher, M. Brown, J. Jacquemier, P. Viens, C. G. Kleer, S. Liu, A. Schott, D. Hayes, D. Birnbaum, M. S. Wicha and G. Dontu, *Cell Stem Cell*, 2007, **1**, 555–567.

25 G. Dontu, W. M. Abdallah, J. M. Foley, K. W. Jackson, M. F. Clarke, M. J. Kawamura and M. S. Wicha, *Genes Dev.*, 2003, **17**, 1253–1270.

26 S. A. Mani, W. Guo, M. J. Liao, E. N. Eaton, A. Ayyanan, A. Y. Zhou, M. Brooks, F. Reinhard, C. C. Zhang, M. Shipitsin, L. L. Campbell, K. Polyak, C. Brisken, J. Yang and R. A. Weinberg, *Cell*, 2008, **133**, 704–715.

27 P. P. Provenzano, K. W. Eliceiri, J. M. Campbell, D. R. Inman, J. G. White and P. J. Keely, *BMC Med.*, 2006, **4**, 38.

28 S. Saha, X. Duan, L. Wu, P. K. Lo, H. Chen and Q. Wang, *Langmuir*, 2012, **28**, 2028–2034.

29 J. P. Chute, G. G. Muramoto, J. Whitesides, M. Colvin, R. Safi, N. J. Chao and D. P. McDonnell, *Proc. Natl. Acad. Sci. U. S. A.*, 2006, **103**, 11707–11712.

30 M. S. Wicha, C. Ginestier, E. Charaffe-Jauffret, F. I. Tarpin, G. Dontu and F. Iovino, *Clin. Exp. Metastasis*, 2008, **25**, 11.

31 Y. Wang, H. Zhe, P. Gao, N. Zhang, G. Li and J. Qin, *Dis. Esophagus*, 2012, **25**, 560–565.

32 A. K. Croker, D. Goodale, J. Chu, C. Postenka, B. D. Hedley, D. A. Hess and A. L. Allan, *J. Cell. Mol. Med.*, 2009, **13**, 2236–2252.

33 R. W. Storms, A. P. Trujillo, J. B. Springer, L. Shah, O. M. Colvin, S. M. Ludeman and C. Smith, *Proc. Natl. Acad. Sci. U. S. A.*, 1999, **96**, 9118–9123.

34 B. A. Reynolds and R. L. Rietze, *Nat. Methods*, 2005, **2**, 333–336.

35 G. G. Jinesh, W. Choi, J. B. Shah, E. K. Lee, D. L. Willis and A. M. Kamat, *Cell Death Differ.*, 2012, **20**, 382–395.

36 S. Okumura-Nakanishi, M. Saito, H. Niwa and F. Ishikawa, *J. Biol. Chem.*, 2005, **280**, 5307–5317.

37 J. Zhang, Q. Liang, Y. Lei, M. Yao, L. Li, X. Gao, J. Feng, Y. Zhang, H. Gao, D. X. Liu, J. Lu and B. Huang, *Cancer Res.*, 2012, **72**, 4597–4608.

38 J. Stingl, P. Eirew, I. Ricketson, M. Shackleton, F. Vaillant, D. Choi, H. I. Li and C. J. Eaves, *Nature*, 2006, **439**, 993–997.

39 P. K. Lo, D. Kanojia, X. Liu, U. P. Singh, F. G. Berger, Q. Wang and H. Chen, *Oncogene*, 2012, **31**, 2614–2626.

40 K. R. Yu, S. R. Yang, J. W. Jung, H. Kim, K. Ko, D. W. Han, S. B. Park, S. W. Choi, S. K. Kang, H. Scholer and K. S. Kang, *Stem Cells*, 2012, **30**, 876–887.

41 J. L. Horning, S. K. Sahoo, S. Vijayaraghavalu, S. Dimitrijevic, J. K. Vasir, T. K. Jain, A. K. Panda and V. Labhasetwar, *Mol. Pharmaceutics*, 2008, **5**, 849–862.

42 F. Xu and K. J. Burg, *Cytotechnology*, 2007, **54**, 135–143.

43 E. Tomaskovic-Crook, E. W. Thompson and J. P. Thiery, *Breast Cancer Res.*, 2009, **11**, 213.

44 J. P. Thiery, *Nat. Rev. Cancer*, 2002, **2**, 442–454.

45 M. Oft, J. Peli, C. Rudaz, H. Schwarz, H. Beug and E. Reichmann, *Genes Dev.*, 1996, **10**, 2462–2477.

46 R. L. Brown, L. M. Reinke, M. S. Damerow, D. Perez, L. A. Chodosh, J. Yang and C. Cheng, *J. Clin. Invest.*, 2011, **121**, 1064–1074.

47 P. Ye, M. A. Nadkarni and N. Hunter, *Biochem. Biophys. Res. Commun.*, 2006, **349**, 229–235.

48 M. H. Chen, G. W. Yip, G. M. Tse, T. Moriya, P. C. Lui, M. L. Zin, B. H. Bay and P. H. Tan, *Mod. Pathol.*, 2008, **21**, 1183–1191.

49 K. Vuoriluoto, H. Haugen, S. Kiviluoto, J. P. Mpindi, J. Nevo, C. Gjerdrum, C. Tiron, J. B. Lorens and J. Ivaska, *Oncogene*, 2011, **30**, 1436–1448.

50 M. H. Yang and K. J. Wu, *Cell Cycle*, 2008, **7**, 2090–2096.

51 J. I. Lopez, J. K. Mouw and V. M. Weaver, *Oncogene*, 2008, **27**, 6981–6993.

52 R. G. Wells and D. E. Discher, *Sci. Signaling*, 2008, **1**, pe13.

53 P. J. Wipff, D. B. Rifkin, J. J. Meister and B. Hinz, *J. Cell Biol.*, 2007, **179**, 1311–1323.

54 O. H. Ocana, R. Corcoles, A. Fabra, G. Moreno-Bueno, H. Acloque, S. Vega, A. Barrallo-Gimeno, A. Cano and M. A. Nieto, *Cancer Cell*, 2012, **22**, 709–724.

55 K. J. Livak and T. D. Schmittgen, *Methods*, 2001, **25**, 402–408.